WEP Warwick Evans Publishing

International Journal of Computer Science and Information Technology

ISSN: 3005-9682 (Print), ISSN: 3005-7140 (Online) | Volume 3, Number 3, Year 2024
DOI: https://doi.org/10.62051/ijcsit.v3n3.02
Journal homepage: https://wepub.org/index.php/IJCSIT/index

Analysis of a Non-Line-of-Sight Indoor Wireless Optical Communication Channel Model

Ke Xiong [1], Hao Wang[1, *], Pengzhang Yu [2]

[1] College of Electronic and Information, Southwest Minzu University, Chengdu, China

[2] Key Laboratory of Electronic Information Engineering, Southwest Minzu University, Chengdu, China

*Corresponding Author: 1942842945@qq.com

ABSTRACT

Wireless Optical Communication (WOC) technology is a wireless communication method that uses light as a carrier. Traditional WOC systems often leverage the direct line-of-sight characteristic for communication, which can lead to issues with alignment between the transmitter and receiver, as well as the arrangement of indoor light sources. The paper introduces a method that employs diffuse reflection of light off indoor walls and ceilings to cover the entire indoor space, with a signal-to-noise ratio (SNR) that ranges from a maximum of 22.6721 to a minimum of 8.5738. This method allows for the receiver and transmitter to be non-stationary, greatly improving the flexibility of the WOC system. The paper studies the channel modeling of the direct link and the first reflection link in indoor WOC systems, and conducts simulation analysis of received power, signal-to-noise ratio, and impulse response in indoor space using an LED array.

KEYWORDS

Indoor Wireless Optical Communication; Channel; Simulation

1. INTRODUCTION

Wireless Optical Communication has the advantages of abundant frequency band resources, no electromagnetic interference, energy conservation and environmental protection, and high security [1-2]. Wireless Optical Communication mainly utilizes the characteristics of Light Emitting Diodes (LEDs) that can switch quickly and are easy to modulate, emitting high-speed modulated optical carrier signals that propagate wirelessly through the air. The light can travel through direct and reflected paths, reaching photoelectric devices such as PIN photodiodes and APD avalanche photodiodes at the receiving end, and then the signal is transmitted through subsequent amplification, filtering, and demodulation to achieve signal transmission. At present, there is a lot of research on indoor wireless optical communication channel modeling, but most of it is based on the direct line-of-sight characteristic for communication, which requires target alignment when in use. This research constructs a direct channel model for indoor wireless optical communication using the micro-element modeling method and employs a recursive approach to process the diffusely reflected light at the micro-element level, thus constructing a channel model for a single reflection.

Indoor Wireless Optical Communication channel modeling technology has achieved significant results. For instance, in 2021, Chenglong Dong proposed a study. The study on the design of light source layouts in indoor visible light communication systems has simulated and analyzed the relationship between layout design and the distribution of received optical power at the model's optimal number of LEDs, offering an optimal solution for indoor light source layout. With a larger number of light sources, genetic algorithms are employed to optimize the light source devices. The optimized light source layout can minimize the variation in optical power on the receiving plane, enhancing communication quality [3]. In 2012, a modeling approach was presented in the document [4] suggesting that the channel response of diffuse reflection be approximated by an exponential function. This approach simplifies the model, but the outcomes may be influenced as a result. Khalifeh and others conducted research on how the distribution of LEDs affects rooms of varying sizes, designed a visible light communication (VLC) system, and utilized a precise ray tracing algorithm to model the communication system [5]. Upon validation, it was confirmed that the system satisfies the requirements set by the international lighting organization regarding indoor illuminance and bit error rate, and the system was employed for the transmission of video signals.

In light of the aforementioned studies, the paper introduces a channel model for wireless optical communication that utilizes a single LED array, which is directed towards the ceiling. The light is then diffusely reflected by the ceiling, allowing its optical power to cover the entire indoor area. MATLAB simulation modeling is employed to simulate and analyze the received power, signal-to-noise ratio, and impulse response within the indoor space.

2. WIRELESS OPTICAL COMMUNICATION CHANNEL MODEL

Figure 1 illustrates the channel diagram of a wireless optical communication system. The transmitting end of the communication system sends the modulated optical signal, which undergoes attenuation and noise superposition through the indoor channel and reaches the receiving end.

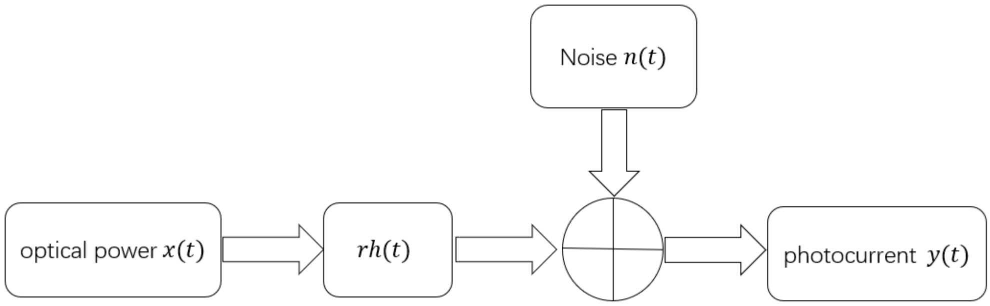

Figure 1 Indoor Wireless Optical Communication Model

In indoor wireless optical communication systems, the mathematical expression of the channel model is shown in Equation (1) [6]:

$$y(t) = rx(t) \otimes h(t) + n(t) \tag{1}$$

$x(t)$ represents the optical signal transmitted by the communication system. γ represents the response efficiency of a PIN photodiode. $h(t)$ represents the system's impulse response. $n(t)$ represents Gaussian white noise. $\otimes$ represents the convolution operation, $y(t)$ represents the output photocurrent.

3. WIRELESS OPTICAL COMMUNICATION CHANNEL LINK

In indoor wireless optical communication, the communication link methods are categorized into two types: line-of-sight (LOS) links and non-line-of-sight (NLOS) links. Figure 2 illustrates the path diagram for LOS links in indoor optical communication, while Figure 3 shows the path diagram for NLOS links in indoor communication.

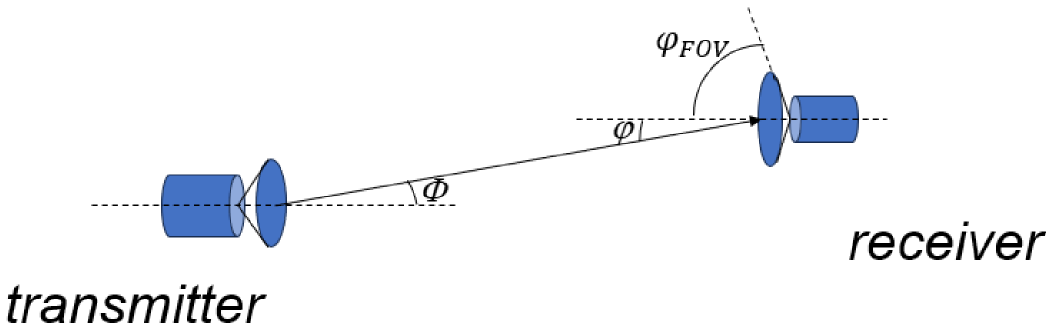

Figure 2. Schematic Diagram of LOS Path

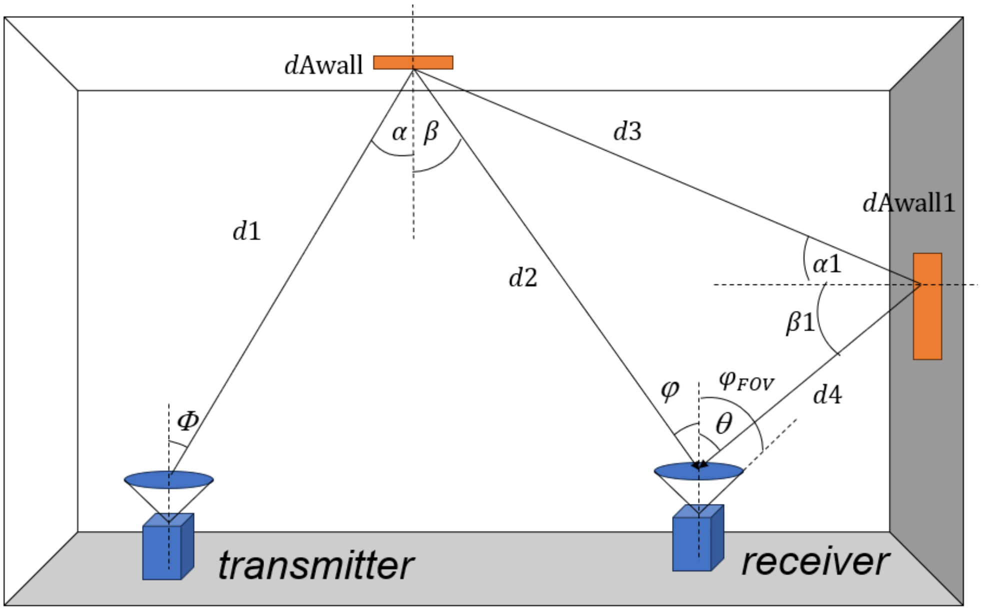

Figure 3. Schematic Diagram of NLOS Path

In wireless optical communication, the line-of-sight (LOS) link, also referred to as a direct link, indicates that the light emitted from the light source reaches the receiver directly without any reflection, refraction, or interference from obstacles. The non-line-of-sight (NLOS) link, also known as an indirect link, means that the light emitted from the source cannot directly reach the receiver and must undergo one or multiple reflections off walls to get to the receiver.

In wireless optical communication systems, the power of the direct light constitutes over 90% of the total received signal power. However, its utilization necessitates target calibration, and any positional deviation or the presence of obstacles between the transmitter and receiver can cause the signal to be interrupted. Thus, the article will leverage non-line-of-sight links for communication. Within NLOS links, there are occurrences of single, double, and multiple reflections, and their light power coverage is significantly broader than that of direct links, addressing the issue of limited mobility during LOS communication. Nevertheless, the multiple reflections in NLOS wireless optical communication can introduce multipath effects, which impact the system's communication speed.

4. CHANNEL THEORY ANALYSIS AND COMPUTATION

Establishing a model for indoor wireless optical communication, the LOS direct channel of the link is depicted in Figure 2, and the NLOS channel is shown in Figure 3. The environmental scenario defined in this paper is an empty room, which includes an LED array as a light source, a photodetector (PD), ceiling, and floor, etc. The dimensions of the room are 5m by 5m by 3m. In the modeling, the light source is positioned at the center of the room, with the photodetector (PD) located on a receiving plane 1 meter above the ground. The position vector of the light source is (2.5, 2.5, 1), the emitted power of the LED array is 1200mW, the wall reflectivity is 0.7, the half-power angle is 30°, the effective receiving area of the receiving plane is $1cm^2$, the receiving field of view (FOV) is 70°, and the Lambertian radiation coefficient is set to 1, indicating an ideal Lambertian light source.

4.1. Channel Impulse Response

The channel impulse response, as an important indicator to characterize the properties of indoor wireless optical communication systems, is frequently utilized to analyze signal distortion and inter-symbol interference issues arising from multipath effects. In the context of indoor wireless optical communication systems, they are typically regarded as linear time-invariant (LTI) systems, and the channel impulse response aptly articulates the fundamental characteristics of the system. The impulse response of the LOS path is illustrated in Equation (2).

$$h_{LOS}(t) = \frac{(m+1)Ar}{2\pi d^2}\cos^m(\Phi)g(\varphi)Ts(\varphi)\cos(\varphi)rect(\varphi/\varphi_{FOV})\delta(t-\frac{d}{c}) \tag{2}$$

In the equation, m represents the Lambertian radiation coefficient. Ar represents the area of the detector. Ts represents the gain of the optical filter. d the distance from the LED to the receiving detector. $\emptyset$ represents LED radiation angle. φ represents the angle of incidence of the light. φ_{FOV} represents the field of view (FOV) of the receiver. c represents speed of light. δ represents Dirac delta function, $rect$ represents a rectangular function as shown in Equation (3), g represents the concentration gain coefficient of a PIN photodiode is shown in Equation (4):

$$rect(x) = \begin{cases} 1 & |x| \le 1 \\ 0 & |x| > 1 \end{cases} \tag{3}$$

$$g(\varphi) = \begin{cases} \frac{n^2}{\sin^2 \varphi_{FOV}} rect(\varphi/\varphi_{FOV}) \end{cases} \tag{4}$$

In this context, n represents the refractive index of the optical concentrator.

As illustrated in Figure 2, with the LED array and the receiver located on a direct line-of-sight (LOS) link, the receiver is 2 meters horizontally distant from the transmitter, and it is 2 meters away from the center of the transmitter. The impulse response for the direct path is shown in Figure 4. The numerical value of the impulse response component for the LOS path is 6.25×10^{-6}, Its transmission delay is 9.4ns.

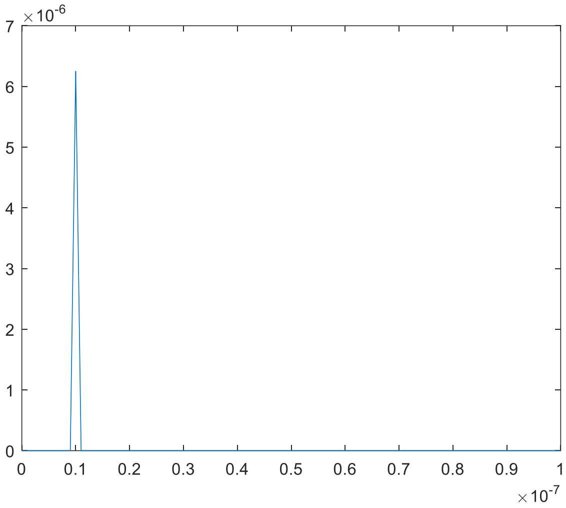

Figure 4. The impulse response of the LOS path

Figure 3 shows the non-line-of-sight (NLOS) link at the receiver, which encompasses a single reflection off the ceiling and a secondary reflection off the walls. The micro-element method is first employed to model the first reflection channel of the NLOS link communication, segmenting the wall into distinct rectangular micro-elements and determining the impulse response from the transmitter to each micro-element on the wall surface. Subsequently, each wall micro-element is treated as an independent light source for the secondary Lambertian radiation; ultimately, the receiving plane is divided into rectangular micro-elements for reception. The impulse response of the first reflection in the NLOS link at the receiver is depicted in Equation (5).

$$h_{NLOS}(1) = \cos^m(\Phi) g(\varphi) Ts(\varphi) \cos(\varphi) rect(\varphi / \varphi_{FOV}) * \cos\alpha \cos\beta \delta(t - \frac{d_1}{c}) \delta(t - \frac{d_2}{c}) \int_{walls} \frac{(m+1)Ar}{2\pi^2 d_1^2 d_2^2} \rho dAwall \tag{5}$$

In the equation, ρ denotes the reflection coefficient of the walls within the room, $d1$ refers to the distance from the LED emission unit to the point of reflection on the wall, $d2$ is the distance from the reflection point to the reception point, α represents the angle between the emitted light ray and the wall's normal, β denotes the angle between the light ray after reflection from the wall and the wall's normal, and $dAwall$ is the area of the micro-element on the reflective surface area of the wall.

Subsequently, the idea of recursive methods is employed to calculate the impulse response of the double reflection, segmenting the light from the first reflection off the wall into independent micro-elements as Lambertian light source models. Upon the second reflection from the wall, the wall is once more divided into micro-elements, with each micro-element on the wall acting as an independent light source for the tertiary Lambertian radiation. The impulse response of the second reflection in the non-line-of-sight (NLOS) link at the receiver is depicted in Equation (6).

$$h_{NLOS}(2) = \cos^m(\Phi) g(\theta) Ts(\theta) \cos(\theta) rect(\theta / \varphi_{FOV}) \cos\alpha 1 \cos\beta 1 \cos\alpha \cos\beta \; \delta(t - \frac{d_1}{c}) \delta(t - \frac{d_3}{c})(t - \frac{d_4}{c}) \int_{wall1} \int_{walls} \frac{(m+1)Ar}{2\pi^3 d_1^2 d_3^2 d_4^2} \rho dAwalldAwall1 \tag{6}$$

In the given formula, θ denotes the angle of incidence of the light ray following the second reflection, $\alpha 1$ signifies the angle between the light ray after the first reflection and the wall's normal, $\beta 1$ indicates the angle between the light ray following the second reflection off the wall and the normal to the wall at the second reflection point, $d3$ is the distance from the first reflection micro-element to the second reflection point on the wall, $d4$ represents the distance from the second reflection point to the receiving point, $dAwall1$ is the area of the micro-element on the wall's surface for the second reflection.

With the vector position of the light source being (2.5, 2.5, 1) and that of the receiver being (0.5, 0.5, 1), the impulse response for the single-reflection NLOS path is depicted in Figure 5. The numerical value of the impulse response component for the single-reflection NLOS path is 2.2164×10^{-7}, with the transmission delay increased to 19 nanoseconds (ns). Adding the impulse response for the double-reflection path as shown in Figure 6, the numerical value of the impulse response component for the double-reflection NLOS path is 9.877×10^{-8}, with the transmission delay increased to 26 nanoseconds (ns). It is evident that light rays traveling along different paths can impact the communication speed. Theoretically, a communication carrier frequency higher than 142 MHz would result in severe inter-symbol interference, greatly increasing the bit error rate. However, in practical use, the bandwidth of high-power LEDs does not exceed 100 MHz, thus the interference due to the system's multipath effects can be disregarded.

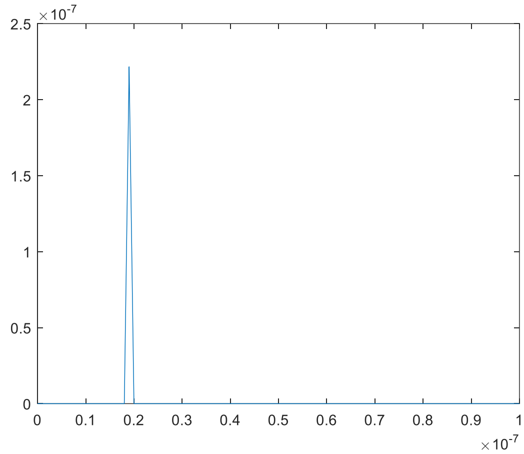

Figure 5. The impulse response of the first reflection path

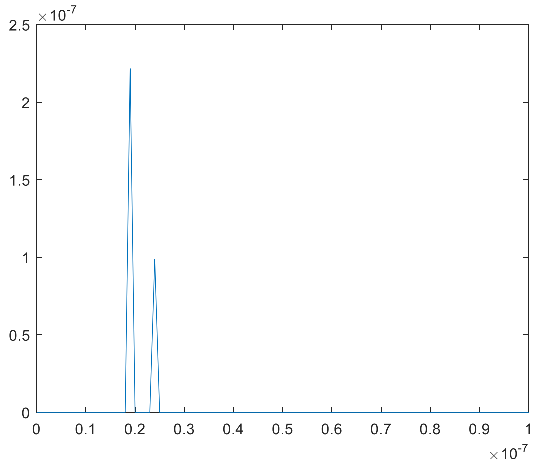

Figure 6. The impulse response of the first reflection path plus the second reflection path

4.2. Channel DC Gain and Received Power

The direct current (DC) gain of a channel is used to describe the extent of signal attenuation along the transmission path. The relationship between the DC gain of the signal and the channel impulse response is commonly represented by the formula (7):

$$H(0) = \int_{-\infty}^{+\infty} h(t)dt \tag{7}$$

In the LOS (Line-of-Sight) link, the formula for the channel's direct current (DC) gain is presented in Equation (8):

$$H_{LOS}(0) = \frac{(m+1)A_r}{2\pi d^2} \cos^m(\Phi) g(\varphi) \cos(\varphi) rect(\varphi / \varphi_{FOV}) T_S(\varphi) \tag{8}$$

The received optical power for the line-of-sight (LOS) link in an indoor wireless optical communication system is represented by Equation (9):

$$P(LOS) = P_t H_{LOS}(0) \tag{9}$$

In the equation, Pt represents the transmitted power.

In the non-line-of-sight (NLOS) link, the direct current (DC) gain is:

$$\begin{aligned} H_{NLOS} &= \cos(\alpha)\cos(\beta)\cos^m(\Phi) g(\varphi)\cos(\varphi) \bullet \\ & T_S(\varphi) rect(\varphi / \varphi_{FOV}) \int_{Wall} \frac{(m+1)A_r}{2\pi^2 d_1^2 d_2^2} \rho dAwall \end{aligned} \tag{10}$$

In an indoor wireless optical communication system, the received optical power for the non-line-of-sight (NLOS) link is represented by Equation (11).

$$P(NLOS) = P_t H_{NLOS} \tag{11}$$

Without accounting for any reflections from obstacles, the MATLAB simulation software is utilized to simulate and analyze the distribution of received power for the LOS (Line-of-Sight) direct path. The power distribution is depicted in the following figure (7). Given a 2-meter separation between the transmitter and receiver, the receiver's maximum received power is 0.9867mw, and the minimum received power is 0.0079mw. There is a considerable disparity between the maximum and minimum optical power, with the power distribution being quite concentrated. The signal-to-noise ratio is high in the vicinity of the optical spot and diminishes with distance from it. The power drops off quickly between different locations. Because the emission angle is fixed, the LOS link's coverage area is limited, necessitating the optimization of layout with multiple LED arrays. As a result, the positions of the transmitter and receiver are relatively static, which is less convenient for use.

In the NLOS (Non-Line-of-Sight) link, the MATLAB simulation software is employed to simulate and analyze the received power of the first reflection of the transmitter's light. The distribution of the received power is illustrated in Figure (8). When the transmitter is situated at the center of the room, the receiver receives greater light power the closer it is to the center, reaching a maximum of 0.0148mw and a minimum of 0.0018mw. In contrast to the LOS (Line-of-Sight) link, the NLOS link has a lower received power; however, it offers a wider coverage area. Should secondary, tertiary, and multiple reflections from the walls be taken into account, the distribution of light power across the entire indoor space becomes more consistent.

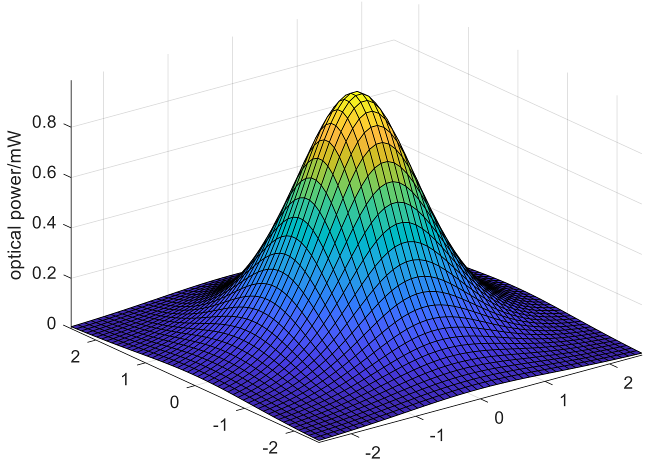

Figure 7. Distribution of Received Optical Power for the LOS Path

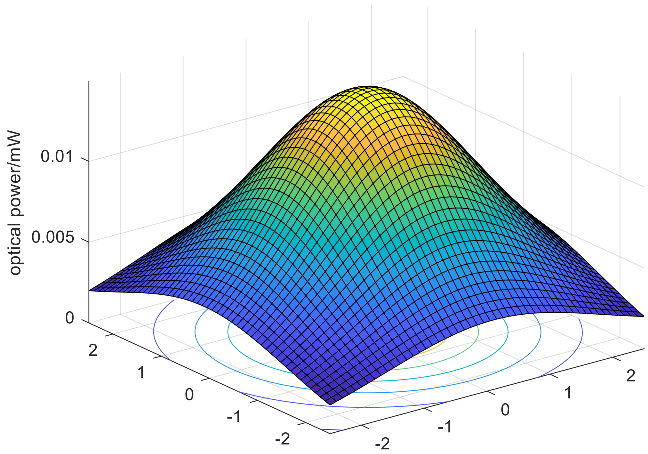

Figure 8. Distribution of Received Optical Power for the NLOS Path

4.3. Channel Signal-to-Noise Ratio (SNR)

The signal-to-noise ratio (SNR) is typically utilized to assess the quality of a system's communication and directly indicates the quality of the received signal. The signal component within the SNR is represented by Equation (12) [7]:

$$S = \gamma^2 P^2 \tag{12}$$

In the formula for the signal-to-noise ratio (SNR), γ indicates the response coefficient of the photoelectric device, and P signifies the power of the received signal.

During communication, noise interferes with the signal, causing distortion and the transmission of erroneous information, impeding the normal flow of communication. However, noise is omnipresent and hard to eliminate in the process of communication transmission. It is considered that noise in indoor WOC systems is typically Additive White Gaussian Noise (AWGN), primarily made up of shot noise, thermal noise, and inter-symbol interference noise. Shot noise is a significant source of noise, arising from the stochastic arrival of photons at the detector, and its magnitude is related to the intensity of the signal light. Thermal noise is composed of the noise from feedback resistors and channel noise. Inter-symbol interference noise mainly results from the multipath effect in wireless optical communication systems, where high-speed signals are delayed along different paths, and when the delay exceeds the signal's pulse interval, overlapping signals lead to inter-symbol interference, thus treating the energy from multiple reflections as noise. The formula for shot noise is presented in Equation (13).

$$\sigma^2{}_{shot} = 2q\gamma PB + 2qI_{bg}I_2B \tag{13}$$

In the formula for noise, q indicates the elementary charge (the quantity of charge of an electron), B is the equivalent noise bandwidth of the receiving circuit, I_{bg} is the dark current (the current that flows through the detector without light), and I_2 represents the noise bandwidth factor, which takes into account the noise shaping and can differ based on the noise properties of the system.

In indoor visible light communication (VLC), the formula for expressing thermal noise is given by:

$$\sigma^2{}_{thermal} = \frac{8\pi kT_k}{G}\eta ArI_2B^2 + \frac{16\pi^2 kT_k\Gamma}{g_m}\eta^2 Ar^2 I_3B^3 \tag{14}$$

In the given formula k represents the Boltzmann constant. T_k signifies the absolute temperature. G is the open-loop voltage gain. η is the inherent capacitance per unit area of the PIN photodiode. Γ denotes the channel noise factor of the field-effect transistor. gm indicates the transconductance of the field-effect transistor. $I3$ is the noise bandwidth factor.

The total noise in an indoor wireless optical communication system can be translated as:

$$N = \sigma^2{}_{thermal} + \sigma^2{}_{shot} + \gamma^2 P^2{}_{ISI} \tag{15}$$

In the context of indoor wireless communication systems, where P_{ISI} denotes the power of inter-symbol interference, the signal-to-noise ratio (SNR) can be expressed as follows, as referenced in:

$$SNR = \frac{S}{N} = \frac{\gamma^2 P^2}{\sigma^2{}_{thermal} + \sigma^2{}_{shot} + \gamma^2 P^2{}_{ISI}} \tag{16}$$

The simulation parameters for the system's signal-to-noise ratio are presented in Table 1. Utilizing the simulation parameters from Table 1, the SNR for both the LOS and NLOS link systems under the LED array is simulated using MATLAB software. The distribution of the SNR from the LOS link simulation is depicted in Figure 9. The distribution of the SNR from the NLOS link simulation is illustrated in Figure 10.

Table 1. Signal-to-Noise Ratio (SNR) Simulation Parameters

parameter name	parameter value
q(charge of an electron)	1.6e-19
B (bandwidth of the system)	100Mbps
I_{bg} (dark current)	300pA
I_2(the noise bandwidth factor)	0.562
γ (responsivity of the photoelectric device)	0.55A/W
k (the Boltzmann constant)	1.38e-23
T_k (absolute temperature)	295K
G (the open-loop voltage gain)	10
η (the inherent capacitance per unit area of the PD)	120pF/cm
Γ (he channel noise factor of the field-effect transistor)	1.5
gm (the transconductance of the field-effect transistor)	30mS
$I3$ (the noise bandwidth factor)	0.0868

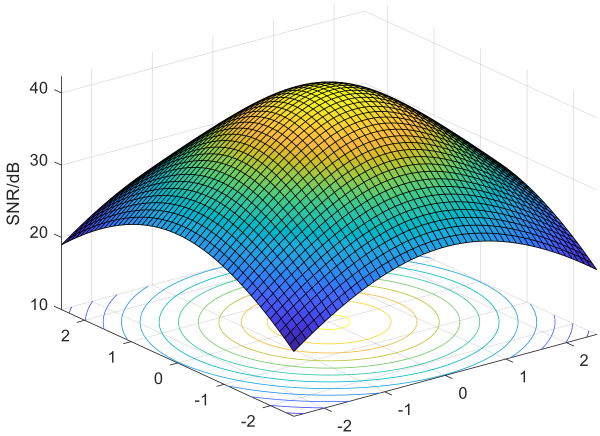

Figure 9. Distribution of Signal-to-Noise Ratio for the LOS Link

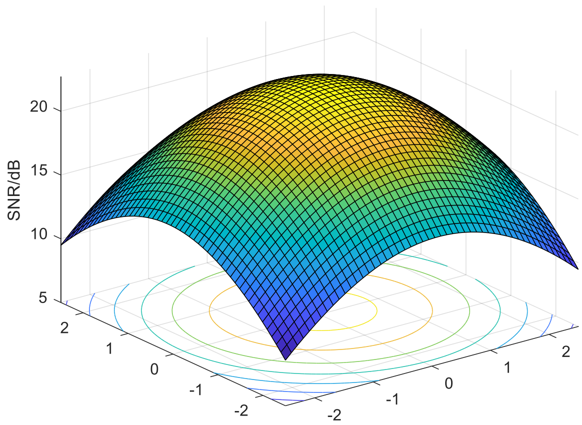

Figure 10. Distribution of Signal-to-Noise Ratio for the NLOS Link

Figure 9 indicates that in the LOS link, the system's SNR correlates with the distribution of the received optical power. The SNR is higher as one gets closer to the center, reaching a maximum of 42.2689 and a minimum of 18.9651. Figure 10 shows that in the NLOS link, the system's SNR is lower compared to the LOS link, with the maximum being 22.6721 and the minimum 8.5738.

5. CONCLUSION

The paper introduces a technique that utilizes diffuse reflection of light off indoor walls and the ceiling to illuminate the entire indoor space. It examines the impulse response, received power, and distribution of signal-to-noise ratio for the indoor wireless optical communication system. Simulations confirm the impulse response of the NLOS link, which exhibits a 7-nanosecond delay between its primary and secondary reflection paths. The highest received power recorded is 0.0148mw, while the lowest is 0.0018mw, The signal-to-noise ratio reaches a maximum of 22.6721dB. and a minimum of 8.5738dB. The system's flexibility is significantly enhanced since the receiver and transmitter are not required to be stationary during communication.

REFERENCES

[1] Y. Celik, "Indoor Visible Light Communication and Positioning with Pan-Tilt Receiver," 2022 Innovations in Intelligent Systems and Applications Conference (ASYU), Antalya, Turkey, 2022, pp. 1-5, doi: 10.1109/ASYU56188.2022.9925550.

[2] GUANGYUN L I, SENZHEN S U N, LI W, et al. Research and Application of Indoor Visible Light Communication Positioning Technology [J]. Acta Geodaetica et Cartographica Sinica, 2022, 51(06):909-924.

[3] C. Dou, C. Wang, T. Mi, Z. Zhang, J. Yang and J. Ao, "Design and Simulation of light Source Layout of Indoor Visible Light Communication System," 2021 4th International Conference on Information Communication and Signal Processing (ICICSP), Shanghai, China, 2021, pp. 523-527, doi: 10.1109/ICICSP54369.2021.9611832.

[4] DING J, HUANG Z, JI Y. Evolutionary Algorithm Based Power Coverage Optimization for Visible Light Communications [J]. IEEE Communications Letters, 2012, 16(04):439-441.

[5] KHALIFEH A, ALAKAPPAN K, SATHISH KUMAR B K, et al. A Simulation Analysis of LEDs' Spatial Distribution for Indoor Visible Light Communication [J]. Wireless Personal Communications, 2022, 122(02):1867-1890.

[6] MIRAMIRKHANI F, UYSAL M. Channel Modelling for Indoor Visible Light Communications [J]. Philosophical Transactions of the Royal Society A, 2020, 378(2169):2019-2027.

[7] LEE K, PARK H, BARRY J R, et al. Indoor Channel Characteristics for Visible Light Communications [J]. IEEE Communications Letters, 2011, (15):217-219.